PHYSICAL REVIEW D **84,** 095017 (2011)

Formalism and upper limits for spin-dependent cross sections in dark matter elastic scattering with nuclei

M. Cannoni

Departamento de Física Aplicada, Facultad de Ciencias Experimentales, Universidad de Huelva, 21071 Huelva, Spain

(Received 24 August 2011; published 11 November 2011)

We revise the spin-dependent neutralino-nucleus elastic scattering comparing the formalisms and approximations found in literature for the momentum transfer dependent structure functions. We argue that one of the normalized structure functions of Divari, Kosmas, Vergados, and Skouras is all that one needs to correctly take into account the detailed nuclear physics information provided by shell-model calculations. The factorization of the particle physics degrees of freedom from the nuclear physics momentum dependent structure functions implied by this formalism allows for a better understanding of the so-called model independent method for setting upper limits. We further discuss the possibility of experiments with spin-dependent sensitivity like COUPP to test or set limits on the proton spin-dependent cross section in the framework of the stau coannihilation region of the constrained minimal supersymmetric standard model. For this model with $A_0 = 0$, we provide a fitting formula by which it is possible to convert an upper limit on the spin-independent cross section as a function of the neutralino mass directly into an exclusion plot in the $(m_{1/2}, \tan\beta)$ plane.

DOI: 10.1103/PhysRevD.84.095017 PACS numbers: 95.35.+d, 12.60.Jv

I. INTRODUCTION

The nature of nonbaryonic dark matter that seems to constitute the largest part of the matter in the Universe is still unknown. If dark matter is formed by nonrelativistic weakly interacting massive particles (WIMP) distributed in the halo of the galaxy, they should scatter elastically with the nuclei in a terrestrial detector [1]. A characteristic signal of the WIMP interaction is the presence of an annual modulation in the event rate correlated with the motion of the Earth [2].

Experimental evidence of this modulation has been reported in the past years by the DAMA collaboration [3], and recently, also by the CoGENT collaboration [4]. The interpretation of these signals favors a light WIMP with mass around 10 GeV and a large spin-independent (SI) WIMP-nucleon cross section of the order of 10^{-4} pb [5]. Other experiments, CDMS [6], XENON100 [7], and SIMPLE [8], that anyway are not sensitive to the annual modulation, have reported upper limits that challenge the values of the cross section and mass statistically favored by DAMA and CoGENT.

If on the experimental side the situation is at least controversial [9,10], on the theoretical side it is not less ambiguous. In the popular scheme of the minimal supersymmetric standard model (MSSM) with R-parity conservation where the lightest neutralino is a natural WIMP candidate, it is possible to accommodate a light neutralino with a cross section able to explain DAMA and CoGENT results while not contradicting other phenomenological constraints [11–14].

In supersymmetric models with unification conditions like the constrained MSSM (CMSSM) light neutralinos with such a large spin-independent cross section are excluded by other experimental constraints such as the LEP bound on the chargino mass. On the other hand, global fits that take into account accelerator, flavor physics, and dark matter constraints, single out best fit points of the parameter space with a heavy neutralino [15–17].

In this paper we thus consider a region of the CMSSM parameter space, the so-called stau coannihilation region ($\tilde{\tau}_{\mathrm{CR}}$). In particular, we are interested to find out if present and future experiments can constrain this region by the spin-dependent (SD) elastic scattering.

In the case of WIMP like the lightest neutralino (or any candidate with the same structure of coupling with nucleons), setting constraints on the SD couplings is, confronted with the SI case, complicated by the fact that: (a) there are two elementary cross sections, WIMP-proton and WIMP-neutron, that in principle should be constrained at the same time and in a way that does not depend on the neutralino ''composition'' (the SI proton and neutron cross sections are to a very good approximation equal); (b) in the formula for the neutralino-nucleus cross section the particle physics degrees of freedom are not factorized from the momentum dependent spin structure functions (SSF), thus when setting upper limits one is forced to fix the neutralino composition by the ratio of the couplings. Actually, problem (b) is at the root of problem (a).

A solution to the problem (a) has been proposed in Ref. [18]. Thereafter the method has become the standard way to derive limits on the SD WIMP-nucleon cross sections and to combine them from different experiments [19,20].

We have discussed problem (b) in a previous paper [21] where it is evidenced that the foreseen factorization is

actually achieved by simply normalizing the standard structure functions to their value at zero momentum transfer.

Here we show that the solution of problem (b) indeed gives a better understanding of the solution to the problem (a) proposed by Ref. [18]. In particular, we show that there is no need of the assumptions made in Ref. [18] that were the object of criticisms Refs. [22,23]. The method is not limited to the zero momentum transfer cross section but actually can incorporate the full momentum dependent structure functions. This is done in Sec. III.

In Sec. II, and in the Appendix, we discuss various aspects of the momentum transfer dependent formalism and argue that some unnecessary complications of the standard formalism are at the origin of the aforementioned problems.

In Sec. IV we then discuss to what extent the limits on the single WIMP-nucleon cross sections derived by actual experiments like COUPP and XENON100 can constraint the $\tilde{\tau}_{\rm CR}$.

In Sec. V we give a parametrization of the SI neutralino-nucleon cross section in the stau-coannihilation region that allows one to translate an experimental upper limit into a bound in the $(m_{1/2}, \tan\beta)$ plane.

The summary and conclusions are given in Sec. VI. In the Appendix we provide a detailed derivation of the formulas discussed in Sec. II.

II. SD FORMALISM REVISED

A. Structure functions and "form factors"

Direct detection experiments employing odd nuclei with nonzero ground state angular momentum J aim to constrain, in the case of absence of a positive signal, the spin-spin interaction of dark matter particles with the nucleons. Detailed nuclear shell-model calculations of the spin matrix elements in the zero momentum transfer limit (ZMTL), i.e. pointlike nucleus, and of the SSF that account for the momentum transfer dependence response, have been carried out for many nuclei employed in actual experiments, see [24] for reviews.

The differential neutralino-nucleus cross section, as a function of the recoil energy of the nucleus $E_R = q^2/2m_A$ being q the modulus of the momentum transfer, has the general form

$$\frac{d\sigma_A^\lambda}{dE_R} = \frac{m_A}{2\mu_A^2 v^2}\sigma_A^\lambda(0)\Phi^\lambda(E_R). \tag{1}$$

Here $\lambda = \mathrm{SI}$ or $\lambda = \mathrm{SD}$, m_A is the mass of the nucleus with mass number A, μ_A the neutralino-nucleus reduced mass, and v the relative velocity. $\sigma_{(A)}^\lambda(0)$ are the ZMTL total cross sections, to be discussed below. The function $\Phi^\lambda(E_R)$ accounts for the structure of the nucleus and is normalized to one in the ZMTL, $\Phi^\lambda(0) = 1$.

For $\lambda = \mathrm{SI}$, $\Phi^{\rm SI}(E_R) = F^2(E_R)$, where $F(E_R)$ is the nuclear form factor. In Eq. (1), therefore, the nuclear physics is separated from the particle physics.

For $\lambda = \mathrm{SD}$, in the standard formalism introduced by Engel in Ref. [25] (see [24,26,27] for reviews), we have

$$\Phi_E^{\rm SD}(E_R) = \frac{S(E_R)}{S(0)}, \tag{2}$$

with

$$S(E_R) = a_0^2 S_{00}(E_R) + a_0 a_1 S_{01}(E_R) + a_1^2 S_{11}(E_R). \tag{3}$$

$i, j = 0, 1$ are isospin indexes and a_0 and a_1 the isoscalar and isovector WIMP-nucleon scattering amplitudes written in the isospin basis. The ZMTL of the functions $S_{ij}(E_R)$ is $S_{ij}(0) \neq 1$, they are not normalized to one and the function S_{01} for some nuclei can be negative. Particle physics and nuclear physics are not separated.

These unpleasant features of the standard formalism are avoided with the formalism of Divari, Kosmas, Vergados, and Skouras [28]. In this framework we can write

$$\Phi_V^{\rm SD}(E_R) = \frac{\mathcal{F}(E_R)}{\mathcal{F}(0)}, \tag{4}$$

with

$$\mathcal{F}(E_R) = a_0^2 F_{00}(E_R) + 2a_0 a_1 F_{01}(E_R) + a_1^2 F_{11}(E_R). \tag{5}$$

Note that in this case $F_{ij}(0) = 1$ by construction. In Ref. [21] (see also [28–30]) we have remarked that the functions $F_{ij}(E_R)$ are practically identical in the recoil energy interval of interest for experiments, not only for light nuclei but also for medium-heavy and heavy nuclei,

$$F_{00}(E_R) \simeq F_{01}(E_R) \simeq F_{11}(E_R). \tag{6}$$

Thanks to Eq. (6), Eq. (5) reduces to

$$\Phi_V^{\rm SD}(E_R) = F_{11}(E_R). \tag{7}$$

Hence, the SD "form factor" is determined by only one SSF. It does not depend anymore on the neutralino properties as it happens in the SI scattering.

The two formalisms are equivalent and connected by

$$F_{ij}(E_R) = \frac{S_{ij}(E_R)}{S_{ij}(0)}. \tag{8}$$

If the S_{ij} are known also the F_{ij} are known and vice versa. Equation (7), anyway, allows for a drastic simplification of the formulas while retaining the exact informations of nuclear shell-model calculations. In literature, in spite of this, the formalism is largely overlooked. In some cases phenomenological parametrizations are used.

One example is the parametrization given in [31,32]

$$F_{\rm LS}(qr_n) = \begin{cases} \left(\frac{\sin(qr_n)}{qr_n}\right)^2 & qr_n < 2.55,\ qr_n > 4.5, \\ 0.047 & 2.55 \le qr_n \le 4.5, \end{cases} \quad (9)$$

with the nuclear radius $r_n \simeq 1.0A^{1/3}$ fm.

Another example is furnished by the parametrization implemented in the code MICROMEGAS [33] for the case of nuclei for which the S_{ij} are not available:

$$F_{\rm mO} = \frac{S_{ij}(q)}{S_{ij}(0)} = \exp\left(-\frac{q^2R_A^2}{4}\right), \quad (10)$$

where $R_A = 1.7A^{1/3} - 0.28 - 0.78(A^{1/3} - 3.8 + [(A^{1/3} - 3.8)^2 + 0.2]^{1/2})$. These expressions are used also in recent literature [8,34,35] even in the case that the functions S_{ij} or F_{ij} are known. It is thus interesting to compare them with F_{11}.

Figure 1 shows the normalized SSF F_{11}, $F_{\rm LS}$, and $F_{\rm mO}$ for one light nucleus, ^{19}F, one medium-heavy, ^{73}Ge, and one heavy nucleus, ^{127}I, all of them largely employed in current experiments. The function F_{11} for ^{19}F is taken from Ref. [28], for ^{73}Ge is obtained from the function S_{11} of Ref. [36], for ^{127}I from the function S_{11} of Ref. [37] (set calculated with the Bonn A potential).

In the abscissas, we use the dimensionless variable $y = (qb/2)^2$, where $b = 1$ fm$A^{1/6}$ is the oscillator size parameter. This variable is the natural one employed in shell-model calculations using harmonic oscillator wave functions. The functional form of S_{ij} and F_{ij} is typically a polynomial or a polynomial times an exponential in y or $u = 2y$ [24,28]. The recoil energy is easily found to be related to y by $E_R = 80 \times y \times A^{-4/3}$ MeV. For clearness we report also the corresponding recoil energies for each nucleus on a second abscissa. The interval $0 < y < 1$ covers the recoil energies interval accessible experimentally but in the case of fluorine the relevant region is only up to $y \sim 0.1$.

The approximation furnished by $F_{\rm LS}$ is reasonable both at low recoil energies and at higher energies in the region of the plateau, especially for the heavy nucleus. This is not surprising, for this parametrization was introduced [31] to fit the SSF in Xe and Nb [25,38]. The approximation furnished by $F_{\rm mO}$ is much worse in all the cases. A different Gaussian parametrization is given, for example, in Refs. [39,40].

We stress again that, for the nuclei for which the functions F_{ij} or S_{ij} have been published, there is no need of phenomenological fits or parametrization. The normalized function F_{11} accounts for the results of the most accurate spin structure function calculations and at the same time allows one to separate the nuclear physics from the particle physics in SD the cross section.

B. Differential and total event rate

In SD scattering, given the neutralino-proton and neutralino-neutron cross sections $\sigma^{\rm SD}_{p,n} = (\mu_p^2/\pi)3|a_{p,n}|^2$, the total cross section at $q = 0$ reads

$$\sigma^{\rm SD}_A(0) = \left(\frac{\mu_A}{\mu_p}\right)^2 \frac{1}{3}\left(\Omega_p(0)\sqrt{\sigma^{\rm SD}_p} + \varrho\Omega_n(0)\sqrt{\sigma^{\rm SD}_n}\right)^2. \quad (11)$$

μ_p is WIMP-proton reduced mass and

$$\Omega_{p,n}(0) = 2\sqrt{\frac{J+1}{J}}\langle \mathbf{S}_{p,n}\rangle \quad (12)$$

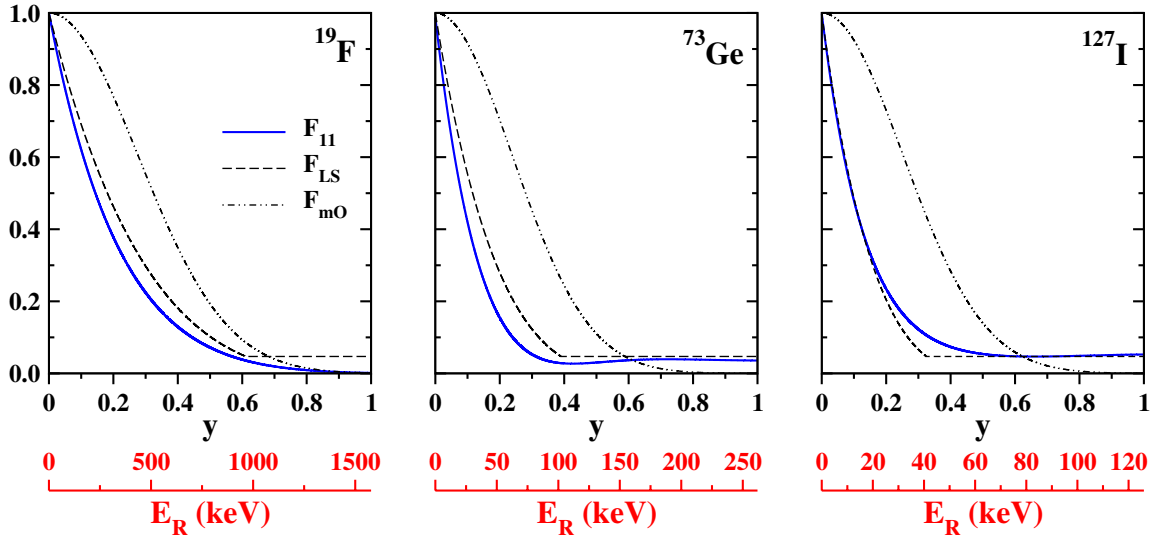

FIG. 1 (color online). In blue line the normalized structure function $F_{11} = S_{11}(q)/S_{11}(0)$, for the nuclei ^{19}F, ^{73}Ge, and ^{127}I. The dashed line refers to the parametrization of Eq. (9) and the dash-dotted line to the parametrization of Eq. (10). The variable in the abscissas is $y = (qb/2)^2$, being q the momentum transfer and $b = 1$ fm$A^{1/6}$ the oscillator size parameter. In the red abscissas the corresponding values of the recoil energies in keV are given.

are the spin matrix elements of the proton and neutron groups. We remind that $\langle \mathbf{S}_{p,n} \rangle \equiv \langle J, M_J = J | S^z_{p,n} | J, M_J = J \rangle$. In general, both the SD WIMP-nucleon scattering amplitudes a_p and a_n [$a_{p,n} = (a_0 \pm a_1)/2$] and the nuclear matrix elements can have opposite sign, hence $\varrho = \pm 1$ is the relative sign between $|\Omega_p(0) a_p|$ and $|\Omega_n(0) a_n|$. An *ab initio* derivation of the SD cross sections using the formalism of Ref. [28] is given in the Appendix.

In the SI case, for the neutralino we have $\sigma_p^{\rm SI} \simeq \sigma_n^{\rm SI} \equiv \sigma^{\rm SI}$, the standard total cross section at $q = 0$ is

$$\sigma_A^{\rm SI}(0) = \left(\frac{\mu_A}{\mu_p}\right)^2 A^2 \sigma^{\rm SI}. \tag{13}$$

The differential recoil rate is obtained by folding Eq. (1) with the velocity distribution function. We use the standard truncated Maxwellian [32]:

$$\begin{aligned} f_1(v) &= \frac{v}{v_0 v_E} f(v), \\ f(v) &= \frac{1}{\kappa}\left[\exp\left(-\frac{(v - v_E)^2}{v_0^2}\right) - \exp\left(-\frac{(v + v_E)^2}{v_0^2}\right)\right], \\ \kappa &= \sqrt{\pi}\,\mathrm{erf}(z) - 2z \exp(-z^2), \\ z &= \frac{v_{\rm esc}}{v_0}. \end{aligned} \tag{14}$$

$v_{\rm esc}$ is the escape velocity, v_0 the velocity of the Sun, and v_E the velocity of the Earth.

Taking $\rho_0 = 0.3\ \mathrm{GeV/cm^3}$ as the local dark matter density density, $\epsilon_0 = 2\mu_A v_0^2 (\mu_A/m_A)$ the typical recoil energy, and $\Phi^{\rm SI} = F^2(E_R)$, $\Phi^{\rm SD} = F_{11}(E_R)$, we can write

$$\frac{dR^\lambda}{dE_R} = \frac{\rho_0 v_0}{m_\chi m_A} \sigma_A^\lambda(0) \frac{dt^\lambda}{dE_R}, \tag{15}$$

$$\frac{dt^\lambda}{dE_R} = \frac{\Phi^\lambda(E_R)}{\epsilon_0} \int_{v_{\rm min}(E_R)}^{v_{\rm max}} \frac{dv}{v_E} f(v). \tag{16}$$

The total rate is simply given by

$$R^\lambda = \frac{\rho_0 v_0}{m_\chi m_A} \sigma_A^\lambda(0) t^\lambda, \tag{17}$$

$$t^\lambda = \int_{E_1}^{E_2} dE_R \frac{dt^\lambda}{dE_R}. \tag{18}$$

The integration limits are $v_{\rm min}(E_R) = v_0\sqrt{E_R/\epsilon_0}$, $v_{\rm max} = v_{\rm esc}$, $E_1 = E_{\rm th}$, $E_2 = \min(E_2^{\rm exp}, E_{\rm max})$, where the maximal recoil energy is $E_{\rm max} = \epsilon_0 (v_{\rm max}/v_0)^2$. The energy threshold $E_{\rm th}$ and $E_2^{\rm exp}$ give the energy interval chosen by an experiment to analyze the data. For comparison with a given experiment using specified nuclei and detection methods, if necessary, one should account in the previous formulas for the energy resolution and efficiencies that may depend on the energy.

In the following we use the Helm form factor in the parametrization proposed in Ref. [32]:

$$\begin{aligned} F^2(q) &= \left(3\frac{j_1(qr_n)}{qr_n}\right)^2 \exp(-q^2 s^2), \\ j_1(x) &= \frac{\sin x}{x^2} - \frac{\cos x}{x}, \\ r_n &= \sqrt{c^2 + \frac{7}{3}\pi^2 a^2 - 5s^2}\ \mathrm{fm}, \\ s &= 0.9\ \mathrm{fm}, \\ a &= 0.52\ \mathrm{fm}, \\ c &= (1.23 A^{1/3} - 0.6)\ \mathrm{fm}. \end{aligned} \tag{19}$$

In literature one can find other parametrization [41] or form factors obtained directly by shell-model calculations [28,29,42]. We use here Eq. (19) because it is employed practically by all the experimental groups.

III. MODEL INDEPENDENT UPPER LIMITS

As an application of the previous formalism we discuss the so-called model independent method for setting upper limits on neutralino cross sections and give an alternative proof of Eq. (13) of Ref. [18].

Let us consider a nucleus such that the SI rate is negligible compared to the SD one: in supersymmetric models the SD rate roughly dominates in nuclei with mass number $A \leq 20$ while SI dominates at larger mass numbers due to A^2 proportionality [27]. We return on this point in the next section.

We introduce the factors

$$\phi_A = \frac{\rho_0 v_0}{m_\chi m_A}, \tag{20}$$

$$\mathcal{C}_A^{p,n} = \frac{\mu_A}{\mu_p} \frac{\Omega_{p,n}(0)}{\sqrt{3}}. \tag{21}$$

Equation (17), with the aid of Eqs. (11), (20), and (21), thus becomes

$$R^{\rm SD} = \phi_A \left(\mathcal{C}_A^p \sqrt{\sigma_p^{\rm SD}} \pm \mathcal{C}_A^n \sqrt{\sigma_n^{\rm SD}}\right)^2 t_A^{\rm SD}. \tag{22}$$

If an experiment with exposure $\mathcal{E}_A = M_A \times T$ (M_A is the mass of the element with mass number A and T the time of live data taking) has no statistically significant evidence, then an upper limit (UL) at some confidence level is put on the number of events N^{UL}. For each unknown m_χ this is converted in an upper limit on the cross section requiring $R \times \mathcal{E} < N^{UL}$, that is,

$$\left(\mathcal{C}_A^p \sqrt{\sigma_p^{\rm SD}} \pm \mathcal{C}_A^n \sqrt{\sigma_n^{\rm SD}}\right)^2 < \frac{N^{UL}}{\phi_A t_A^{\rm SD} \mathcal{E}_A}. \tag{23}$$

The right-hand side of (23) is by definition the experimental upper limit on the neutralino-nucleus SD cross section, let us call $\sigma_A^{\rm lim}$ as in Ref. [18],

$$\sigma_A^{\rm lim} \equiv \frac{N^{UL}}{\phi_A t_A^{\rm SD} \mathcal{E}_A}. \tag{24}$$

Furthermore, utilizing the same name of Ref. [18], we define the quantities

$$\sigma_{p,n}^{\rm lim(A)} \equiv \frac{\sigma_A^{\rm lim}}{(\mathcal{C}_A^{p,n})^2}. \tag{25}$$

Dividing both members of (23) by (24) and using the quantities (25), we arrive at

$$\left(\frac{\sqrt{\sigma_p^{\rm SD}}}{\sqrt{\sigma_p^{\rm lim(A)}}} \pm \frac{\sqrt{\sigma_n^{\rm SD}}}{\sqrt{\sigma_n^{\rm lim(A)}}} \right)^2 < 1, \tag{26}$$

that is exactly Eq. (13) of Ref. [18] in the case of the allowed region in the (σ_p, σ_n) plane.

In Ref. [18] the nucleon cross section limits in Eq. (25) are defined as basic quantities that then are combined to give Eq. (26). To do this it is necessary to assume that for a given nucleus it is possible to set separately limits on the SD-proton and SD-neutron cross sections even in the case that one contribution is clearly subdominant. These assumptions and the method were criticized in Refs. [22–24].

In reality our derivation shows that such hypotheses are unnecessary and that the full justification of Eq. (26) only relies on the factorization of the particle physics from nuclear physics degrees of freedom and has a general validity.[1]

Another common misunderstanding about Eq. (26) is that it is based on ZMTL total cross section and that it does not take into account the exact momentum dependent structure function.

Actually, we see that using F_{11}, the correct behavior of the SSF can be taken into account in the upper limit $\sigma^{\rm lim(A)}$ by the factor $t^{\rm SD}$, see Eq. (24).

On the other hand, the ''upper limits'' on the single proton or neutron cross sections, Eq. (25), are just useful quantities introduced to write Eq. (23) in the compact form (26). They become the actual experimental upper limits if, for the nucleus from which these are determined and in a specific WIMP model, one can prove that the proton contribution is dominant over the neutron contribution or vice versa (given the dominance of the SD rate over the SI rate). In general, the exclusion curves on the single cross sections are fundamentally indicative of the experiment's sensitivity and cannot constrain particle physics models in a universal way.

[1]This result was also implicitly obtained, with different notations and considering the case of general phases, in Ref. [30].

IV. SD SCATTERING AND THE $\tilde{\tau}_{\rm CR}$

To further clarify the last point, we choose a specific particle physics model, that is the constrained minimal supersymmetric standard model (CMSSM) with R-parity conservation. We consider the parameter space with fixed trilinear scalar coupling $A_0 = 0$, positive Higgs mixing term ($\mu > 0$) which is the benchmark supersymmetric theory for phenomenological and experimental studies [43]. If the neutralino is required to furnish the cosmological relic density inferred by WMAP [44], then, for fixed $\tan\beta$ only specific regions in the $(m_{1/2}, m_0)$ plane are left. In the ($\tilde{\tau}_{\rm CR}$) the lightest stau is almost degenerate in mass with the neutralino and the coannihilation of the two particles in the early Universe brings the value of the relic density in the favored WMAP interval. This parameter space is still untouched by direct detection experiments and LHC just started to explore it [15–17]; moreover, it will be hard to probe it with indirect detection methods such as γ ray from neutralino annihilation in the halos [45–47].

The strips in the plane $(m_{1/2}, m_0)$ [43] for varying $\tan\beta$ from 10 to 50 in steps of 5, are shown in the inset of Fig. 2(a). The strips and the cross sections are obtained with DARKSUSY [48], imposing WMAP constraints on the relic density $0.096 < \Omega h^2 < 0.128$, accelerator constraints on the lightest Higgs, $m_h > 114$ GeV and chargino mass $m_{\chi_1^+} > 103.5$ GeV and the flavor physics constraint from bottom quark radiative transitions.

In the same figure the SI neutralino-proton cross section as a function of the neutralino mass is shown. The SD neutralino-proton and neutralino-neutron cross section are shown in Fig. 2(b) and in the inset of Fig. 2(b), respectively. Two general features are worth noting: the SI cross section depends on $\tan\beta$ more strongly than the SD cross sections, the former varying by an order of magnitude and the latter by a factor less than 2; the SD are $\mathcal{O}(10^2)$ larger than the SI, in agreement with [49].

The neutralino field in the mass basis can be written as $\chi_1^0 \equiv N_{11}\tilde{B} + N_{12}\tilde{W}^0 + N_{13}\tilde{H}_1 + N_{14}\tilde{H}_2$, where N_{1i} are the elements of the matrix that diagonalizes the neutralino mass matrix, $\tilde{B}$, $\tilde{W}^0$ are the neutral gaugino fields, and $\tilde{H}_1$, $\tilde{H}_2$ the neutral Higgsino fields. In all the considered parameter space the neutralino is bino-like: we find numerically $N_{11} \sim 0.99 \gg N_{13} \sim 10^{-3} \gg N_{12}, N_{14}$. This means that the coupling to the Z boson that is driven by the Higgsinos couplings proportional to N_{13} and N_{14} is heavily suppressed; the cross section is determined by squarks exchange. Analogously also in the SI case to the CP-even Higgs h and H are suppressed by N_{13} and N_{14} and the cross sections is thus mainly determined by squark exchange. Anyway, the couplings of the Higgs to down-type quark become $(\tan\beta)^2$ enhanced at large $\tan\beta$. The

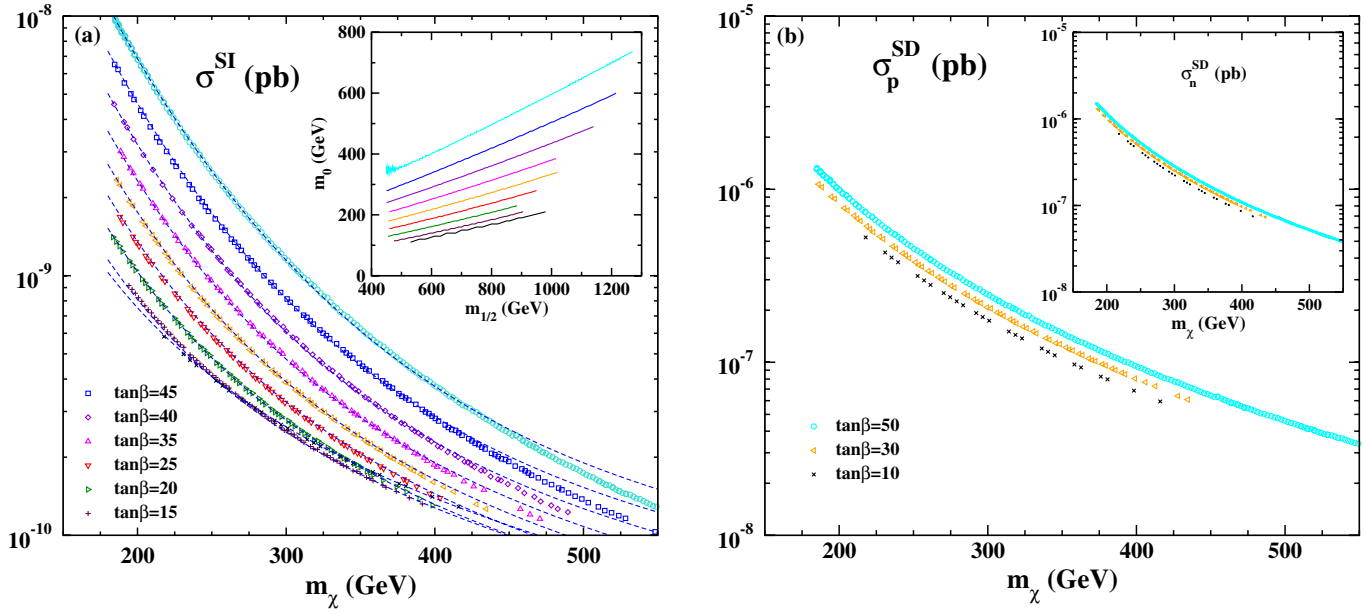

FIG. 2 (color online). (a) Spin-independent neutralino-nucleon cross section in the stau coannihilation region with $A_0 = 0$ and $\tan\beta$ from 10 to 50 in steps of five as a function of the neutralino mass. The dashed line is obtained with the fitting formula, Eq. (29), with coefficients given in Table I. The inset shows for each value of $\tan\beta$ the strip in the plane $(m_{1/2}, m_0)$ allowed by WMAP constraints on the relic density $0.096 < \Omega h^2 < 0.128$ and satisfies accelerator constraints. (b) Spin-dependent neutralino-proton cross section and, in the inset, the spin-dependent neutralino-neutron cross section for $\tan\beta = 10$, 30, and 50.

two contributions thus can be of the same order and SI cross section is more sensitive to variations of $\tan\beta$.

A. ^{19}F, ^{127}I, and the $\tilde{\tau}_{CR}$

To discuss the relation between the SI and SD rates, we consider the light nucleus ^{19}F that is known to furnish the best sensitivity to the proton SD cross section [28,50,51] and ^{127}I, that have both good SI and SD sensitivities.

For ^{19}F, we use the spin matrix elements of Ref. [28] that give $\Omega_p^{19}(0) = 1.646$ and $\Omega_n^{19}(0) = -0.030$. In this case the neutron contribution in the SD rate can be safely neglected. We remark that the first nuclear shell-model calculation for ^{19}F [51] found $\langle \mathbf{S}_p \rangle = 0.441$, $\langle \mathbf{S}_n \rangle = -0.109$. The successive calculation of Ref. [28] using a more realistic interaction found $\langle \mathbf{S}_p \rangle = 0.4751$ and $\langle \mathbf{S}_n \rangle = -0.0087$. The proton contribution is thus similar but the neutron contribution is clearly negligible. The statement that the neutron contribution is relevant, see for example [8], in light of the more accurate calculation of Ref. [28], is doubtful.

As reminded above, for light nuclei like fluorine, the SD rate can be dominant over the SI, but this has to be checked in each particular WIMP model. We show the ratio R^{SD}/R^{SI} for fluorine in Fig. 3(a). The SD rate is bigger by a factor up more than 2 at low and medium $\tan\beta$ but it is smaller than the SI rate at large $\tan\beta$; in any case the two rates are always of the same order of magnitude. The SI rate cannot be completely neglected at high $\tan\beta$ and for lower $\tan\beta$, neglecting it, one underestimates the total rate (see Ref. [52] for the case of general MSSM). The exclusion plots in the (m_χ, σ_p^{SD}) are inaccurate for the $\tilde{\tau}_{CR}$. In this case, one has to draw an exclusion plot in the $(\sigma_p^{SD}, \sigma^{SI})$ plane for each fixed mass, the so-called mixed coupling approach [53].

Nuclear shell-model calculations give for ^{127}I $\Omega_p^{127}(0) = 0.731$ and $\Omega_n^{127}(0) = 0.177$ (spin matrix elements obtained with the potential Bonn A from Ref. [37]). Although proton favoring, the neutron group contribution to the nuclear spin is of the same order of magnitude. If the neutralino couplings to the proton and neutron are similar, the neutron contribution to the nuclear spin must be considered. This indeed is what happens in the $\tilde{\tau}_{CR}$, where $0.75 < \sigma_p^{SD}/\sigma_n^{SD} < 0.9$ [21] for $\tan\beta$ between 10 and 50. Furthermore, $a_p < 0$ and $a_n > 0$, thus a cancellation in the SD rate is expected because the products $a_p\langle \mathbf{S}_p \rangle$ and $a_n\langle \mathbf{S}_n \rangle$ are of the same order and have opposite sign. Figure 3(c) shows the ratio of R^{SD}/R^{SI} in ^{127}I only considering the proton contribution, while in Fig. 3(b) both are included. Because of the A^2 proportionality, the SI rate always dominates by a factor from 4 to 25 in Fig. 3(c), but the cancellation makes the SD rate from 2 to 3 orders of magnitude smaller than the SI, Fig. 3(b).

In the case of $\tilde{\tau}_{CR}$, hence, iodine can only constrain the SI interaction. The exclusion plots in the planes (m_χ, σ_p^{SD}), (m_χ, σ_n^{SD}), or the combined $(\sigma_p^{SD}, \sigma_n^{SD})$ at fixed neutralino mass, derived using ^{127}I cannot constrain the $\tilde{\tau}_{CR}$, for they are derived neglecting the dominant SI contribution or the equally important neutron contribution that almost cancels the proton one.

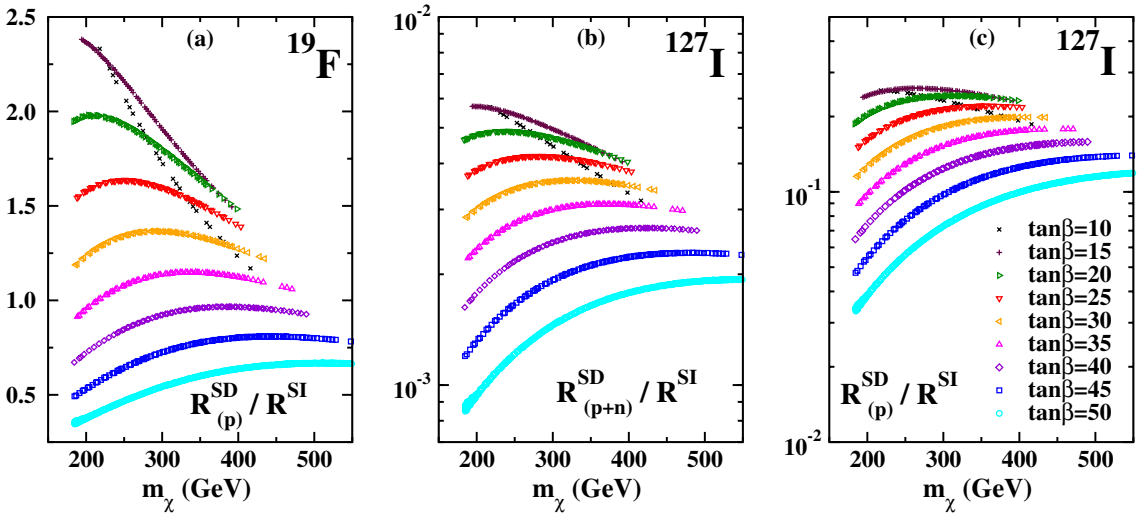

FIG. 3 (color online). Ratio of the spin-dependent total event rate over the spin-independent rate R^{SD}/R^{SI} varying tanβ in the stau coannihilation region of the CMSSM with $A_0 = 0$ and $\mu > 0$. In panel (a) for ^{19}F. In panel (b) the ratio is plotted for ^{127}I taking into account both the proton and neutron contribution in the spin-dependent rate; in panel (c) only the proton contribution is included. The points of the parameter space are the same as in Fig. 2.

B. COUPP and the $\tilde{\tau}_{CR}$

The two nuclei discussed so far are the detecting medium of COUPP [54], a bubble chamber with CF_3I. We use the latest data from Ref. [54]: an affective exposure of CF_3I after cuts of $\mathcal{E} = 28.1$ kg $\times$ days, 50% efficiency, $E_{th} = 21$ keV, $N^{UL} = 6.7$ at 90% confidence level and the same values of the velocities, $v_0 = 230$ km/s, $v_{esc} = 650$ km/s and an average velocity of the Earth $v_E = 244$ km/s. In Fig. 4(a) the blue solid line is the present limit on SD WIMP-proton cross section derived from the fluorine fraction, while in Fig. 4(b) it is the limit on the SI cross section derived from the iodine fraction. The blue-dashed lines are limits extrapolated with the same N^{UL}, 100% efficiency, effective exposure 500 kg $\times$ yr and threshold at 7 keV. The red solid lines are the cross sections for tan$\beta = 50$, the orange ones for tan$\beta = 10$.

The indication that we derive from Fig. 4 is that it will be unlikely for COUPP to probe the $\tilde{\tau}_{CR}$ by SD scattering unless very large exposures of fluorine are achieved. On the other hand, a part of the parameter space will be probed by the SI scattering with iodine. This is not a limitation for the $\tilde{\tau}_{CR}$ since the two cross sections are clearly correlated.

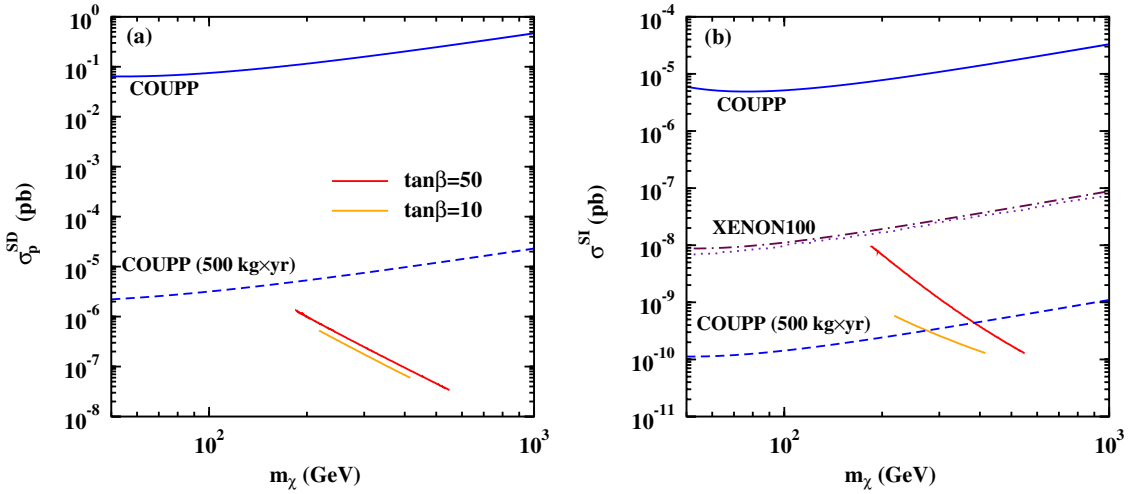

FIG. 4 (color online). (a) Spin-dependent neutralino-proton cross sections for tan$\beta = 10$ (orange line) and 50 (red line) in the stau coannihilation region with $A_0 = 0$, $\mu > 0$. The blue solid line represents the present upper limit from COUPP, the blue-dashed line the extrapolated COUPP limit with an effective exposure of 500 kg $\times$ year and threshold at 7 keV. (b) The same as (a) but for the proton spin-independent cross section. The dash-dotted line is the upper limit from XENON100 calculated as explained in the text, the dotted line the limit published in Ref. [7].

A constraint on $\sigma^{\rm SI}$ automatically implies a constraint on $\sigma^{\rm SD}$. As a matter of fact, should evidence be reported by more experiments and rates measured in fluorine, iodine, and other elements like xenon, argon, or germanium, the full information on the SD sector can be reconstructed [21,55].

As discussed in Sec. IVA, the SI rate in the $\tilde{\tau}_{\rm CR}$ cannot be neglected for fluorine. Considering a mixed SI-SD approach with a fixed neutralino mass, we obtain

$$\sigma_p^{\rm SD} < \sigma_p^{\rm lim(F)} - \frac{(\mathcal{C}_F^{\rm SI})^2 t_F^{\rm SI}}{(\mathcal{C}_F^p)^2 t_F^{\rm SD}} \sigma^{\rm SI}. \tag{27}$$

In analogy with Sec. II we set $\mathcal{C}^{\rm SI} = (\mu_A/\mu_p)A$. At $\tan\beta = 50$, where the SI rate is more important, the correction term on the right-hand side gets values larger than $\sigma_p^{\rm SD}$, in any case the largest values are of order 10^{-6} pb. These values when compared with the present limits, $\sigma_p^{\rm lim(F)} \simeq 10^{-1}$ pb from COUPP and $\simeq 10^{-2}$ pb from SIMPLE [8], are anyway negligible. Hence, one should start to consider the SI rate only when the exposure is such that the sensitivity reaches the values of $\sigma_p^{\rm SD}$ predicted by the model.

V. CONSTRAINING THE ($m_{1/2}$, $\tan\beta$) PLANE

In Fig. 4(b) we also show for comparison the present upper limit of XENON100 [7], which is the most stringent on the SI cross section. To be consistent with COUPP, we have calculated the XENON100 plot using the same values of the velocities given above and the following data: effective exposure of 1471 kg $\times$ days, energy threshold at 8.4 keV, and $N^{UL} = 5.62$ at 90% confidence level deduced by the Feldman-Cousins method [56] with three events observed and mean background 1.8. As for the COUPP limits, we have calculated this curve using the total event rate without energy resolution function. Our curve differs by few percent from the published one, dotted line in Fig. 4(b). The latter is obtained with a statistical analysis of the energy spectrum that takes into account all the experimental uncertainties and with values of the velocities $v_0 = 220$ km/s, $v_{\rm esc} = 544$ km/s, and $v_E = 232$ km/s.

This exercise shows that for masses above 50 GeV the limits are more robust and less sensitive to the experimental details, statistical method to analyze the data and velocities (needless to say this is not true in the low mass region). In the high mass range $m_\chi > 50$ GeV, the exclusion limits are also robust against changes of the velocity distributions [57], being the major source of uncertainty a factor of 2 in ρ_0.

Since we have remarked above that the $\tilde{\tau}_{\rm CR}$ will be probably probed through the SI scattering, we further investigate what kind of information on the $\tilde{\tau}_{\rm CR}$ parameter space can be extracted. We note from Fig. 2(a) that the SI cross section is a smooth decreasing function of the neutralino mass when m_0 and $m_{1/2}$ are varied along the WMAP allowed lines for fixed $\tan\beta$. Clearly it is also a continuous function of this parameter. Therefore we can look for a general fitting formula valid for all the values of $\tan\beta$. We first fit each $\sigma^{\rm SI}$ of Fig. 2(a) for a given value of $\tan\beta$ with the function

$$\sigma = \sum_{k=2}^{4} \mathfrak{s}_k \left(\frac{100\ \text{GeV}}{m_\chi}\right)^k, \tag{28}$$

and than the coefficients $\mathfrak{s}_k$ are fitted with a fourth order polynomial in $\tan\beta$. We thus find

$$\sigma^{\rm SI}(\tan\beta, m_\chi) = \sum_{k=2}^{4} \left[\sum_{i=0}^{4} \sigma_{ki} (\tan\beta)^i \left(\frac{100\ \text{GeV}}{m_\chi}\right)^k \right]. \tag{29}$$

The coefficients of the fit σ_{ki} are given in Table I. The fit obtained with Eq. (29) is shown in Fig. 2(a) with a dashed line.

Analogously, the neutralino mass can be parametrized along the WMAP lines. We find that for all the values of $\tan\beta$ it holds

$$m_\chi \simeq 0.44 m_{1/2} - 15\ \text{GeV}. \tag{30}$$

While the slope 0.44 is found for all the values, the constant negative term is an average value, since it presents a very mild dependence on $\tan\beta$ that anyway is not important for what follows. Thus, using Eq. (30) in Eq. (29) we end up with a formula $\sigma^{\rm SI}(\tan\beta, m_{1/2})$ for the cross section in terms of the fundamental parameters $m_{1/2}$ and $\tan\beta$. In last analysis, this allows one to convert an upper limit on the event rate directly into an exclusion plot in the ($m_{1/2}$, $\tan\beta$) plane.

The result of this procedure is shown in Fig. 5, where the excluded regions are on the left of the curves. The COUPP upper limit with an effective exposure of 500 kg $\times$ year, dashed blue line in Fig. 4(a), corresponds to the dotted black line in Fig. 5. The other curves are obtained for XENON100 considering an effective exposure to be

TABLE I. Coefficients for the fitting formula of Eq. (29).

k	$(\sigma)_{k0}$ (pb)	$(\sigma)_{k1}$ (pb)	$(\sigma)_{k2}$ (pb)	$(\sigma)_{k3}$ (pb)	$(\sigma)_{k4}$ (pb)
2	2.469×10^{-9}	5.085×10^{-11}	5.432×10^{-12}	1.783×10^{-13}	-6.089×10^{-16}
3	2.716×10^{-9}	-9.790×10^{-10}	3.92×10^{-11}	-6.413×10^{-13}	-6.059×10^{-15}
4	1.395×10^{-8}	-2.029×10^{-9}	2.143×10^{-10}	-6.711×10^{-12}	9.481×10^{-13}

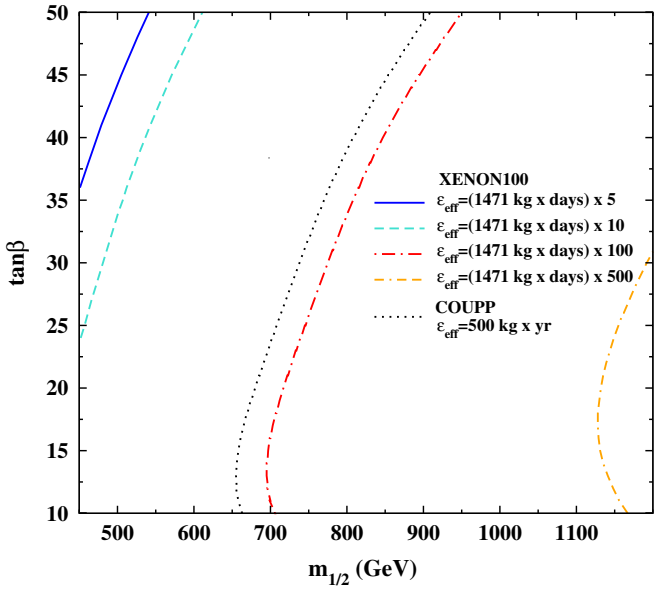

FIG. 5 (color online). Exclusion curves in the plane $(m_{1/2}, \tan\beta)$ for the CMSSM stau coannihilation region with $A_0 = 0$, $\mu > 0$, set by an upper limit on the spin-independent neutralino-nucleon cross section using the fitting formulas Eqs. (29) and (30). The regions to the left of the curves are excluded. The dotted line corresponds to the upper limit of COUPP (500 kg $\times$ yr), dashed blue line in Fig. 4(b). The other lines are extrapolations for XENON100 where the present effective exposure is multiplied by factors 5, 10, 100, and 500.

5, 10, 100, and 500 times the present value of 1471 kg $\times$ days. The dot-dashed red line corresponds roughly to the effective exposure of a future ton mass detector with 1 yr operation and total acceptance cut of 40%. The extrapolation of COUPP, dotted black line, is obtained without any acceptance cut.

We have to remark the limitations of the fitting formula. The coefficients in Table I have many particle physics uncertainties. First of all, the cross section and the relic density were calculated with DARKSUSY with the default values of the hadronic matrix elements. Other codes can give slightly different values of the cross section for the same input parameters. Furthermore, the dependence of the SI cross section on not precisely known hadronic physics quantities can cause variations up to a factor 5 for a given point of the CMSSM parameter space [49]. There is a further dependence of the SI cross section on A_0. Anyway the choice $A_0 = 0$ is the benchmark case study also for direct searches of supersymmetric particles at LHC: ATLAS and CMS typically present exclusion curves in the $(m_0, m_{1/2})$ plane with $A_0 = 0$ and fixed $\tan\beta$ [58,59]. With the proposed formula, hence, one has a direct idea of the sensitivity of a direct detection experiment to one of the cosmologically favored region of the CMSSM parameter space in a complementary way to LHC.

VI. SUMMARY

In this paper we have reviewed the formalisms and the approximations found in literature for the treatment of the SD neutralino-nucleus elastic scattering. We argued that all that one needs to correctly take into account the detailed nuclear physics information provided by shell-model calculations is just one of the normalized structure functions of Ref. [28].

We have shown that the factorization of the particle physics degrees of freedom from the nuclear physics momentum dependent structure functions implied by this formalism allows for a straightforward proof of the general formula (26) proposed in Ref. [18] without the need of the assumptions that were criticized in Ref. [23].

We have further discussed the ability of some of the present experiments and their future upgrade to larger active masses (COUPP and XENON100) to constrain the stau coannihilation region of the CMSSM. In this region of the parameter space the neutralino mass is in the interval 180–550 GeV and the SI cross section is a decreasing function of the mass for $10 < \tan\beta < 50$, taking values in the range 10^{-8}–10^{-10} pb and it is still poorly constrained by experiments. The SD cross sections, with the proton and the neutron, are in the range 10^{-6}–10^{-8} pb.

COUPP, although the high sensitivity of ^{19}F to the proton SD scattering and the fact that the SD neutralino-nucleon cross sections are larger than the SI neutralino-nucleon cross section, can constrain the model in its large mass phase only by the SI interaction with ^{127}I. The reasons are various: first, because of the A^2 scaling of the SI neutralino-nucleus cross section; second, there is a strong cancellation between the proton and neutron contribution in the SD neutralino-^{127}I cross section; third, the active mass of ^{19}F is small.

Furthermore, in ^{19}F, for the considered particle physics model, the SI rate is never negligible compared to the SD rate. In the case that the exposure were such that the model

could be probed through SD scattering, an exclusion curve in the plane $(m_\chi, \sigma_p^{\rm SD})$ would be inaccurate.

Finally, we have given a fitting formula for the SI neutralino-nucleon cross section in the stau coannihilation region as a function of the two fundamental parameters $\tan\beta$ and $m_{1/2}$ ($10 < \tan\beta < 50$) that allows one to directly convert an upper limit into an exclusion plot in the ($\tan\beta$, $m_{1/2}$) plane for the case study $A_0 = 0$.

ACKNOWLEDGMENTS

The author thanks J. D. Vergados and M. E. Gomez for inspiring discussions, suggestions, and comments on the manuscript. P. Gondolo is acknowledged for useful questions during the TeVPA 2011 conference where preliminary results of this paper were presented. Support by MultiDark, Grant No. CSD2009-00064 of the Spanish MICINN project Consolider-Ingenio 2010 Programme and partial support from MICINN Projects No. FPA2009-10773, No. MICINN-INFN(PG21)FPA2009-10773, and from Junta de Andalucia under Grant No. P07FQM02962 are acknowledged.

APPENDIX: PROOF OF THE FORMULAS OF SEC. II

In this Appendix we derive the formulas given in Sec. II following the formalism of Ref. [28] but with a simplified and slightly different notation.

The neutralino-nucleon SD cross section is determined by the axial part of effective Lagrangian. At the nucleon level, in the isospin representation that is convenient for nuclear physics calculations, we can write

$$\mathcal{L}_{\rm eff} = \bar{\chi}\gamma^\mu\gamma^5\chi\bar{N}2s_\mu\tfrac{1}{2}(a_0\mathbb{1} + a_1\hat{\tau}_3)N. \tag{A1}$$

The operator $\hat{\tau}_3$ act as $\hat{\tau}_3|p\rangle = |p\rangle$, $\hat{\tau}_3|n\rangle = -|n\rangle$ and $\mathbb{1}$ is the identity operator in isospin space. Thus, for $N = p, n$ the isospin operator gives $(a_0 \pm a_1)/2 = a_{p,n} = \sum_q d_q \Delta q^{(N)}$, where d_q is the effective coupling with quarks and $\Delta q^{(N)}$ the spin fractions of the nucleon carried by the quarks. We do not discuss further the physics involved at the nucleon level, see Refs. [49,50].

Taking the nonrelativistic limit we get the neutralino-nucleus spin-spin interaction,

$$\hat{V} = 4\hat{\mathbf{s}}_\chi \cdot \sum_{i=1}^{A}\frac{1}{2}(a_0\mathbb{1} + a_1\hat{\tau}_i^3)\hat{\mathbf{S}}_i\delta(\mathbf{r} - \mathbf{r}_i). \tag{A2}$$

Here $\hat{\mathbf{S}}_i$ and $\mathbf{r}_i$ are the spin and coordinates of the ith nucleon. In literature sometimes factors $G_F/\sqrt{2}$, $G_F\sqrt{2}$, or $G_F 2\sqrt{2}$ are extracted from $a_{0,1}$. To simplify the formulas, we adopt instead the convention that all the couplings are included in $a_{0,1}$.

The spin operator of the neutralino operates on eigenstates of the spin $|s\rangle$, while conventionally all the angular momentum operators of the nucleus are evaluated in state with the maximal value of the z projection, $\langle\hat{\mathbf{O}}\rangle \equiv \langle J, M_J = J|\hat{O}^z|J, M_J = J\rangle$. The nuclear wave function depends also on the isospin and the coordinates of the nucleons

$$|A\rangle = |J, M_J = J, \tau_3, \mathbf{r}_1 \ldots \mathbf{r}_A\rangle. \tag{A3}$$

The elastic differential cross section in the center of mass frame and the total cross section, in the case that there is no angular dependence of the amplitude, are given by

$$\frac{d\sigma}{d\Omega} = \frac{\mu_A^2}{4\pi^2}\overline{|\mathcal{M}|^2}, \qquad \sigma = \frac{\mu_A^2}{\pi}\overline{|\mathcal{M}|^2}, \tag{A4}$$

where the scattering matrix element, with $|A, \chi\rangle = |A\rangle|s\rangle$, is

$$\mathcal{M} = \langle A, \chi|\int d\mathbf{r}e^{-i\mathbf{q}\cdot\mathbf{r}}\hat{V}|A, \chi\rangle. \tag{A5}$$

For two spin operators acting on different spaces, the average over the initial directions of modulus squared of the scalar product is $\overline{|\mathbf{S}_a \cdot \mathbf{S}_b|^2} = \frac{1}{3}\mathbf{S}_a^2\mathbf{S}_b^2$, hence,

$$\overline{|\mathcal{M}|^2} = \tfrac{1}{3}16\langle\hat{\mathbf{s}}_\chi^2\rangle_s\langle\hat{\boldsymbol{\Sigma}}^2\rangle_A. \tag{A6}$$

We have defined the operator

$$\hat{\boldsymbol{\Sigma}} = \sum_{i=1}^{A}\frac{1}{2}(a_0\mathbb{1} + a_1\hat{\tau}_i^3)\hat{\mathbf{S}}_i e^{-i\mathbf{q}\cdot\mathbf{r}_i} = \frac{1}{2}(a_0\hat{\boldsymbol{\Omega}}_0 + a_1\hat{\boldsymbol{\Omega}}_1), \tag{A7}$$

with

$$\hat{\boldsymbol{\Omega}}_0 = \sum_{i=1}^{A}\mathbb{1}\hat{\mathbf{S}}_i e^{-i\mathbf{q}\cdot\mathbf{r}_i}, \qquad \hat{\boldsymbol{\Omega}}_1 = \sum_{i=1}^{A}\hat{\tau}_i^3\hat{\mathbf{S}}_i e^{-i\mathbf{q}\cdot\mathbf{r}_i}. \tag{A8}$$

To evaluate $\langle\hat{\boldsymbol{\Sigma}}^2\rangle_A$ we note that for a vector operator, the matrix elements in states $|J, M_J = J\rangle$ are related to the reduced matrix elements by [60]

$$\begin{aligned}\langle J||\hat{\mathbf{O}}||J\rangle &= \frac{\sqrt{J(J+1)(2J+1)}}{J}\langle J, J|\hat{O}^z|J, J\rangle,\\ \langle J, J|\hat{\mathbf{O}}^2|J, J\rangle &= \frac{1}{2J+1}|\langle J||\hat{\mathbf{O}}||J\rangle|^2.\end{aligned} \tag{A9}$$

It follows:

$$\langle J, J|\hat{\mathbf{O}}^2|J, J\rangle = \frac{J+1}{J}|\langle J, J|\hat{O}^z|J, J\rangle|^2. \tag{A10}$$

We thus define the momentum dependent matrix elements,

$$\Omega_0(q) = 2\sqrt{\frac{J+1}{J}}\langle\hat{\Omega}_0^z\rangle_A, \qquad \Omega_1(q) = 2\sqrt{\frac{J+1}{J}}\langle\hat{\Omega}_1^z\rangle_A. \tag{A11}$$

From Eqs. (A7)–(A11), we find

$$\langle \hat{\boldsymbol{\Sigma}}^2 \rangle_A = \frac{1}{16} |a_0 \Omega_0(q) + a_1 \Omega_1(q)|^2. \tag{A12}$$

Obviously, $\langle \hat{\mathbf{s}}_\chi^2 \rangle_s = s(s+1) = 3/4$. Equation (A6) thus takes the form

$$\overline{|\mathcal{M}|^2} = \tfrac{1}{4} |a_0 \Omega_0(q) + a_1 \Omega_1(q)|^2. \tag{A13}$$

Expanding the square and factoring out the zero momentum values, we introduce the normalized structure functions $F_{ij}(q)$:

$$F_{ij}(q) = \frac{\Omega_i(q)\Omega_j(q)}{\Omega_i(0)\Omega_j(0)}, \tag{A14}$$

and find

$$\overline{|\mathcal{M}|^2} = \tfrac{1}{4}(a_0^2 \Omega_0^2(0) F_{00}(q) + 2a_0 a_1 \Omega_0(0)\Omega_1(0) F_{01}(q) + a_1^2 \Omega_1^2(0) F_{11}(q)). \tag{A15}$$

By reason of Eq. (6), we can make the approximation

$$\overline{|\mathcal{M}|^2} \simeq \tfrac{1}{4}(a_0 \Omega_0(0) + a_1 \Omega_1(0))^2 F_{11}(q). \tag{A16}$$

Taking $q = 0$ in Eqs. (A11) and using $\hat{\tau}_3 |p\rangle = +|p\rangle$ and $\hat{\tau}_3 |n\rangle = -|n\rangle$, we have

$$\Omega_0(0) = 2\sqrt{\frac{J+1}{J}} \left\langle \sum_{i=1}^{A} \mathbb{1} \hat{S}_i^z \right\rangle_A = 2\sqrt{\frac{J+1}{J}} (\langle \mathbf{S}_p \rangle + \langle \mathbf{S}_n \rangle) = \Omega_p(0) + \Omega_n(0), \tag{A17}$$

$$\Omega_1(0) = 2\sqrt{\frac{J+1}{J}} \left\langle \sum_{i=1}^{A} \hat{\tau}_3^i \hat{S}_i^z \right\rangle_A = 2\sqrt{\frac{J+1}{J}} (\langle \mathbf{S}_p \rangle - \langle \mathbf{S}_n \rangle) = \Omega_p(0) - \Omega_n(0). \tag{A18}$$

Equation (12) is thus proved.

Furthermore, using $a_{0,1} = a_p \pm a_n$ and Eq. (12), Eq. (A16) becomes

$$\overline{|\mathcal{M}|^2} = 4\frac{J+1}{J} (a_p \langle \mathbf{S}_p \rangle + a_n \langle \mathbf{S}_n \rangle)^2 F_{11}(q). \tag{A19}$$

For a single nucleon (A19) reduces to $3|a_{p,n}|^2$, hence,

$$\sigma_{p,n}^{\mathrm{SD}} = 3\frac{\mu_p^2}{\pi} |a_{p,n}|^2, \tag{A20}$$

Eq. (11) follows from Eqs. (A19) and (A20).

Finally, with the substitution $d\Omega = \frac{4\pi}{4\mu_A^2 v^2} dq^2 = \frac{2m_A \pi}{\mu_A^2 v^2} dE_R$ in Eq. (A4) and using Eqs. (A19) and (11), we obtain Eq. (1).

The present formalism and the standard formalisms are equivalent and connected by

$$S_{ij}(q) = \frac{2J+1}{(1+\delta_{ij})8\pi} \Omega_i(q)\Omega_j(q). \tag{A21}$$

For a given nuclear wave function they furnish the same cross section.

In last analysis, the difference resides in the way by which the multipole decomposition in vector spherical harmonics of the operator (A7) is carried out. In the standard formalism this done in terms of the operator $\mathcal{T}_L^{\mathrm{el5}}$ and $\mathcal{L}_L^5$, see Refs. [24–26] and references therein for explicit formulas and meaning. Both operators contain the couplings a_0 and a_1, thus the modulus squared of each contains terms proportional to a_0^2, a_1^2, and the interference $a_0 a_1$. The function $S(q)$ in terms of the functions $S_{ij}(q)$ arises after a rearrangement of these terms.

In the formalism of Ref. [28], the multipole decomposition in vector spherical harmonics is done on the operators (A8). Anyway, keeping separated the terms in a_0 and a_1 has the advantage that the squared of the amplitude is always a perfect square, see Eq. (A13), and limit $q = 0$ is reached in a more transparent way.

[1] M. W. Goodman and E. Witten, Phys. Rev. D **31**, 3059 (1985).
[2] K. Freese, J. A. Frieman, and A. Gould, Phys. Rev. D **37**, 3388 (1988).
[3] R. Bernabei *et al.* (DAMA/LIBRA Collaboration), Eur. Phys. J. C **67**, 39 (2010).
[4] C. E. Aalseth *et al.* (CoGeNT Collaboration), Phys. Rev. Lett. **107**, 141301 (2011).
[5] D. Hooper and C. Kelso, Phys. Rev. D **84**, 083001 (2011).
[6] Z. Ahmed *et al.* (CDMS-II Collaboration), Phys. Rev. Lett. **106**, 131302 (2011).
[7] E. Aprile *et al.* (XENON100 Collaboration), Phys. Rev. Lett. **107**, 131302 (2011).
[8] M. Felizardo *et al.* (SIMPLE Collaboration), arXiv:1106.3014.
[9] J. I. Collar, arXiv:1103.3481; arXiv:1106.0653; arXiv:1106.3559.
[10] SIMPLE Collaboration, arXiv:1107.1515.
[11] N. Fornengo, S. Scopel, and A. Bottino, Phys. Rev. D **83**, 015001 (2011).
[12] P. Belli, R. Bernabei, A. Bottino, F. Cappella, R. Cerulli, N. Fornengo, and S. Scopel, Phys. Rev. D **84**, 055014 (2011).
[13] D. T. Cumberbatch, D. E. Lopez-Fogliani, L. Roszkowski, R. R. de Austri, and Y. L. S. Tsai, arXiv:1107.1604.
[14] L. Calibbi, T. Ota, and Y. Takanishi, J. High Energy Phys. 07 (2011) 013.

[15] M. Farina, M. Kadastik, D. Pappadopulo, J. Pata, M. Raidal, and A. Strumia, Nucl. Phys. **B853**, 607 (2011).
[16] O. Buchmueller *et al.*, Eur. Phys. J. C **71**, 1722 (2011).
[17] G. Bertone, D. G. Cerdeno, M. Fornasa, R. R. de Austri, C. Strege, and R. Trotta, arXiv:1107.1715.
[18] D. R. Tovey, R. J. Gaitskell, P. Gondolo, Y. A. Ramachers, and L. Roszkowski, Phys. Lett. B **488**, 17 (2000).
[19] F. Giuliani, Phys. Rev. Lett. **93**, 161301 (2004).
[20] F. Giuliani and T. A. Girard, Phys. Rev. D **71**, 123503 (2005).
[21] M. Cannoni, J. D. Vergados, and M. E. Gomez, Phys. Rev. D **83**, 075010 (2011).
[22] V. A. Bednyakov, Phys. At. Nucl. **67**, 1931 (2004).
[23] V. A. Bednyakov and H. V. Klapdor-Kleingrothaus, Phys. Part. Nucl. **40**, 583 (2009).
[24] V. A. Bednyakov and F. Simkovic, Phys. Part. Nucl. **36**, 131 (2005); **37**, S106 (2006).
[25] J. Engel, Phys. Lett. B **264**, 114 (1991).
[26] J. Engel, S. Pittel, and P. Vogel, Int. J. Mod. Phys. E **1**, 1 (1992).
[27] G. Jungman, M. Kamionkowski, and K. Griest, Phys. Rep. **267**, 195 (1996).
[28] P. C. Divari, T. S. Kosmas, J. D. Vergados, and L. D. Skouras, Phys. Rev. C **61**, 054612 (2000).
[29] P. Toivanen, M. Kortelainen, J. Suhonen, and J. Toivanen, Phys. Rev. C **79**, 044302 (2009).
[30] J. D. Vergados, Nucl. Phys. **B829**, 383 (2010).
[31] P. F. Smith *et al.*, Phys. Lett. B **379**, 299 (1996).
[32] J. D. Lewin and P. F. Smith, Astropart. Phys. **6**, 87 (1996).
[33] G. Belanger, F. Boudjema, A. Pukhov, and A. Semenov, Comput. Phys. Commun. **180**, 747 (2009).
[34] H. An, S. L. Chen, R. N. Mohapatra, S. Nussinov, and Y. Zhang, Phys. Rev. D **82**, 023533 (2010).
[35] C. L. Shan, J. Cosmol. Astropart. Phys. 07 (2011) 005.
[36] V. I. Dimitrov, J. Engel, and S. Pittel, Phys. Rev. D **51**, R291 (1995).
[37] M. T. Ressell and D. J. Dean, Phys. Rev. C **56**, 535 (1997).
[38] J. Engel, S. Pittel, E. Ormand, and P. Vogel, Phys. Lett. B **275**, 119 (1992).
[39] P. Gondolo, arXiv:hep-ph/9605290.
[40] G. Bertone, D. Hooper, and J. Silk, Phys. Rep. **405**, 279 (2005).
[41] G. Duda, A. Kemper, and P. Gondolo, J. Cosmol. Astropart. Phys. 04 (2007) 012.
[42] T. S. Kosmas and J. D. Vergados, Phys. Rev. D **55**, 1752 (1997).
[43] J. R. Ellis, K. A. Olive, Y. Santoso, and V. C. Spanos, Phys. Lett. B **565**, 176 (2003).
[44] D. Larson *et al.*, Astrophys. J. Suppl. Ser. **192**, 16 (2011).
[45] M. Cannoni, M. E. Gomez, M. A. Sanchez-Conde, F. Prada, and O. Panella, Phys. Rev. D **81**, 107303 (2010).
[46] M. A. Sanchez-Conde, M. Cannoni, F. Zandanel, M. E. Gomez, and F. Prada, arXiv:1104.3530.
[47] J. Ellis, K. A. Olive, and V. C. Spanos, arXiv:1106.0768.
[48] P. Gondolo *et al.*, J. Cosmol. Astropart. Phys. 07 (2004) 008.
[49] J. R. Ellis, K. A. Olive, and C. Savage, Phys. Rev. D **77**, 065026 (2008).
[50] J. R. Ellis and R. A. Flores, Phys. Lett. B **263**, 259 (1991).
[51] A. F. Pacheco and D. Strottman, Phys. Rev. D **40**, 2131 (1989).
[52] V. A. Bednyakov and F. Simkovic, Phys. Rev. D **72**, 035015 (2005).
[53] R. Bernabei *et al.*, Phys. Lett. B **509**, 197 (2001).
[54] E. Behnke *et al.* (COUPP Collaboration), Phys. Rev. Lett. **106**, 021303 (2011).
[55] M. Pato, arXiv:1106.0743.
[56] G. J. Feldman and R. D. Cousins, Phys. Rev. D **57**, 3873 (1998).
[57] C. McCabe, Phys. Rev. D **84**, 043525 (2011).
[58] G. Aad *et al.* (ATLAS Collaboration), Phys. Lett. B **701**, 186 (2011).
[59] V. Khachatryan *et al.* (CMS Collaboration), Phys. Lett. B **698**, 196 (2011).
[60] L. D. Landau and E. M. Lifshitz, *Quantum Mechanics: Non-Relativistic Theory* (Pergamon Press, Oxford, 1977), 3rd ed.